ISSN 1063-7761, Journal of Experimental and Theoretical Physics, 2011, Vol. 113, No. 2, pp. 266–275. © Pleiades Publishing, Inc., 2011.
Original Russian Text © V.V. Val'kov, S.V. Aksenov, 2011, published in Zhurnal Eksperimental'noi i Teoreticheskoi Fiziki, 2011, Vol. 140, No. 2, pp. 305–316.

ELECTRONIC PROPERTIES OF SOLID

Effects of Inelastic Spin-Dependent Electron Transport through a Spin Nanostructure in a Magnetic Field

V. V. Val'kov[a,b,c,*] and S. V. Aksenov[a,b]

[a] *Institute of Physics, Siberian Branch, Russian Academy of Sciences, Krasnoyarsk, 660036 Russia*
[b] *Siberian Federal University, Krasnoyarsk, 660041 Russia*
[c] *Reshetnikov Siberian State Aerospace University, Krasnoyarsk, 660014 Russia*
**e-mail: vvv@iph.krasn.ru*

Received September 30, 2009; in final form, December 28, 2010

Abstract—The transport properties and current–voltage (I–V) characteristics of a system of spin dimers with antiferromagnetic coupling arranged between metallic contacts are investigated in the tight binding approximation using the Landauer–Buttiker formalism. It is shown that the s–$d(f)$ exchange interaction between the spin moments of the electrons being transported and the spins of the nanostructure leads to the formation of a potential profile as well as its variation due to spin-flip processes. As a result, the spin-dependent transport becomes inelastic, and the transmission coefficient and the I–V characteristic are strongly modified. It is found that the application of a magnetic field induces additional transparency peaks in the spectral characteristic of the system and causes the colossal magnetoresistance effect.

DOI: 10.1134/S1063776111060070

1. INTRODUCTION

Advances in experimental studies on the nanometer scale in recent decades have necessitated a theoretical description of quantum transport in nanostructures. A large number of available publications in this field reflect the considerable effect of transported particles on the conducting properties of nanoobjects. A striking example of this effect is the Coulomb blockade that appears as a result of Coulomb repulsion between electrons in nanoobjects and a tunneling electron [1–3].

In such a situation, transport is largely determined by inelastic processes associated with modification of a structure's potential relief due to interaction with a transported electron. In particular, inelastic effects associated with electron–phonon interaction and strong electron correlations are clearly manifested in the transport characteristics of molecular contacts. The inelastic nature of quantum transport in such structures is responsible for the nonlinear behavior of the I–V characteristics and conductivity, as well as negative differential conductivity, dynamic switching and switching current noise, current hysteresis, heating of a molecular contact, and the emergence of the Kondo resonance [4–7]. Nontrivial properties of conducting molecular contacts make such systems interesting as prospective parts of nanoelectronics devices [8].

The idea of using spin degrees of freedom as additional channels for data storage and transmission has been significantly developed in contemporary experimental and theoretical studies and has facilitated an individual trend known as spin electronics [9, 10]. In this field, inelastic spin–spin interactions also play a significant part. In particular, it is well known that the magnetization of a ferromagnetic nanolayer in zero magnetic field can be controlled via the s–$d(f)$ interaction between the spin moments of conduction electrons and the spin moments of atoms. The action of torque on the magnetization of a ferromagnet was proposed as a mechanism triggering magnetization reversal [11, 12]. Later, a volumetric mechanism of nonequilibrium spin injection was worked out [13, 14]. Other examples of the effect of the inelastic s–$d(f)$ exchange interaction on the conducting properties of nanoobjects are experiments and theory in scanning electron microscopy which investigate the transport properties of single magnetic atoms and their complexes containing a small number of atoms adsorbed on a metal substrate in strong magnetic fields at low temperatures [15–18].

In recent years, transport phenomena relating to molecular electronics as well as spintronics have been intensely investigated. For example, the effect of inelastic spin–spin and electron–phonon interactions in the case of magnetic electrodes are manifested in the electron population, density of states, spin-dependent current, and tunnel magnetoresistance [19, 20]. Thus, analysis of effects of inelastic spin-dependent transport in magnetic nanostructures such as single atoms or clusters on metal surfaces [21] or magnetic molecules [22] appears promising. Such systems may exhibit strong anisotropy sufficient for sustaining stable spin orientation at low temperatures. Considerable

anisotropy of individual atoms in such nanoclusters is interesting as a possible way to reduce magnetic bits to sizes smaller than those at which the domains of modern thin-film magnetic materials become unstable at room temperature. Analysis of the effect of external magnetic field on the conductivity of systems with well-pronounced magnetic anisotropy is of vital importance.

In this paper, we report on the results of calculating the transport characteristics of a nanostructure represented by a system of spin dimers and placed between metal contacts in an external magnetic field. A spin dimer in the ground singlet state with excited triplet states is a widespread configuration of the spin subsystem for a number of molecules and molecular structures. Inelastic scattering of conduction electrons from the potential relief of such a nanostructure appears due to spin–spin s–$d(f)$ exchange interaction between the spin moments of the transported particles and the spin moments of dimers. However, the inelastic scattering in this case does not cause energy dissipation; i.e., transport is coherent and can be described using the Landauer–Buttiker formalism [23, 24].

2. FORMULATION OF THE PROBLEM AND HAMILTONIAN

Let us consider a spin-polarized electron current through two planes of magnetoactive atoms forming a system of spin dimers, which for brevity will be referred to as a setup. We assume that the setup is located between metal electrodes, which in turn are connected to electron reservoirs in the form of macroscopic metallic junctions. The diagram of the setup is shown in Fig. 1. Since reservoirs are macroscopic conductors much larger than the electrodes, the electrons entering a reservoir are thermalized and have the temperature and chemical potential of the junction prior to their return to the setup. Thus, a junction must be reflectionless. This means that an electron incident on the junction is absorbed completely and thermalized prior to its re-emission into the setup [25]. The electrodes are assumed to be ideal and can generally be prepared from various metals.

The further description will be carried out in the tight binding approximation. In addition, we will disregard jumps and exchange interactions in directions perpendicular to the x axis. Thus, the transport of the electron ensemble in the system under investigation is reduced to the passage of an individual particle through an individual 1D chain. The individual chain is formed by the regions of left and right metal electrodes as well as the central part of the nanosetup (spin dimer). In the entire chain, the spacing between the sites is assumed to be the same (a). The Hamiltonian of an individual chain can be written in the form

$$\hat{H} = \hat{H}_L + \hat{H}_R + \hat{H}_{LD} + \hat{H}_{DR} + \hat{H}_{De} + \hat{H}_{sf} + \hat{H}_D + U(n). \quad (1)$$

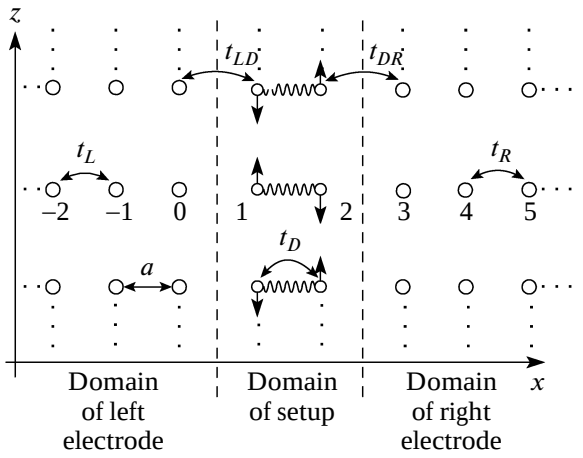

Fig. 1. Profile of a nanosetup including metal junctions.

Here, the first two terms are the electron Hamiltonians L and R of the left and right junctions, respectively, which can be written in the following form in the tight binding approximation in the secondary quantization representation:

$$\hat{H}_L = \sum_{\sigma,\, n=-\infty}^{0} [\varepsilon_{L\sigma} c^+_{n\sigma} c_{n\sigma} + t_L(c^+_{n\sigma} c_{n-1,\sigma} + c^+_{n-1,\sigma} c_{n\sigma})], \quad (2)$$

$$\hat{H}_R = \sum_{\sigma,\, n=3}^{\infty} [\varepsilon_{R\sigma} c^+_{n\sigma} c_{n\sigma} + t_R(c^+_{n+1,\sigma} c_{n\sigma} + c^+_{n\sigma} c_{n+1,\sigma})], \quad (3)$$

where $c^+_{n\sigma}$ ($c_{n\sigma}$) is the production (annihilation) operator for a conduction electron with spin σ at the nth site of the junction α ($\alpha = L, R$), and $\varepsilon_{\alpha\sigma} = \varepsilon_\alpha - g_e \mu_B H\sigma$ and t_α are the one-electron spin-dependent energy at a site in an external magnetic field $\mathbf{H}$ and the hopping integral at the α junction. The z axis is oriented along the magnetic field. The third and fourth terms describe the jumps of a conduction electron between the setup and the junctions,

$$\hat{H}_{LD} = \sum_\sigma t_{LD}(c^+_{1\sigma} c_{0\sigma} + c^+_{0\sigma} c_{1\sigma}), \quad (4)$$

$$\hat{H}_{DR} = \sum_\sigma t_{DR}(c^+_{3\sigma} c_{2\sigma} + c^+_{2\sigma} c_{3\sigma}). \quad (5)$$

The fifth term of the Hamiltonian describes the behavior of electrons in the setup,

$$\hat{H}_{De} = \sum_{\sigma,\, n=1}^{2} [\varepsilon_{D\sigma} c^+_{n\sigma} c_{n\sigma} + t_D(c^+_{2\sigma} c_{1\sigma} + c^+_{1\sigma} c_{2\sigma})]. \quad (6)$$

The inelastic character of electron transport is related to the term $\hat{H}_{sf}$ in the total Hamiltonian (1), which is responsible for the s–$d(f)$ exchange interaction between the spin moments of conduction electrons and the spins of the dimer,

$$\hat{H}_{sf} = \frac{A_{sf}}{2}\sum_{n=1}^{2}[(c_{n\uparrow}^{+}c_{n\downarrow}\hat{S}_n^{-} + c_{n\downarrow}^{+}c_{n\uparrow}\hat{S}_n^{+}) + (c_{n\uparrow}^{+}c_{n\uparrow} - c_{n\downarrow}^{+}c_{n\downarrow})\hat{S}_n^{z}], \quad (7)$$

where A_{sf} is the parameter of the s–$d(f)$ exchange interaction and $\hat{S}_n^{+}$, $\hat{S}_n^{-}$, and $\hat{S}_n^{z}$ are the spin operators of the dimer at the nth site.

Operator $\hat{H}_D$ in Hamiltonian (1) describes the exchange interaction between the spin moments of the dimers in the setup, as well as their Zeeman energy in magnetic field **H**. In the isotropic case, this operator can be written in the form

$$\hat{H}_D = I(\mathbf{S}_1 \cdot \mathbf{S}_2) - g_D\mu_B H(S_1^z + S_2^z), \quad (8)$$

where I is the parameter of the exchange interaction between the dimer spins. From here on, we will assume that $I > 0$. This means that an exchange coupling of the antiferromagnetic type exists between spin moments. Consequently, in relatively weak magnetic fields ($g_D\mu_B H < I$), the ground state of a dimer corresponds to the singlet state.

The last term in the Hamiltonian characterizes the potential energy of electrons in the external electric field produced by potential difference V across the junctions. It is well known that the shape of the I–V characteristic depends to a considerable extent on the specific profile of the potential in the region between the electrodes. For simplicity, we will confine our analysis to the transport characteristics, assuming that the potential varies linearly in the central region.

3. STATIONARY STATES

In writing the solution to the Schrödinger equation, we must take into account the change in the state of the spin dimer, which is induced by the action of an electron flying near it. Analysis of the s–$d(f)$ operator shows that the term proportional to $\sigma^z S^z$ induces the transformation of the dimer from the singlet state D_{00} into the triplet state D_{10} without changing the spin projection of the electron being transported, while the term proportional to $\sigma^- S^+$ is responsible for the transformation of the dimer from singlet state D_{00} to triplet state D_{11} with a simultaneous change in the spin projection of the transported electron. Therefore, the complete Hilbert space is the product of the subspace for the electron being transported and the subspace of the spin dimer. As the basis of the Hilbert space, we choose the basis of states each of which characterizes the spin state of the transported electron at site n, as well as one of the four states of the spin dimer. For this reason, this basis will be denoted as $D_{JJ_z}c_{n\sigma}^{+}|0\rangle$, where D_{JJ_z} corresponds to the state of the spin dimer with the total spin angular momentum J and projection J_z of this angular momentum onto the quantization axis z and $|0\rangle$ is the vacuum state indicating the state of the system without an electron. In the chosen notation, the four states of the dimer are described as

$$D_{00} = \frac{1}{\sqrt{2}}(|\uparrow\downarrow\rangle - |\downarrow\uparrow\rangle),$$
$$D_{10} = \frac{1}{\sqrt{2}}(|\uparrow\downarrow\rangle + |\downarrow\uparrow\rangle), \quad (9)$$
$$D_{11} = |\uparrow\uparrow\rangle, \quad D_{1,-1} = |\downarrow\downarrow\rangle,$$

where we have used the Dirac ket vectors $|\sigma_1\sigma_2\rangle$. Each of these four ket vectors describes a state in which the first spin of the dimer has projection σ_1 and the second, σ_2.

In accordance with the system of notation adopted here, the solution to the Schrödinger equation in the case when the electron transported from the left junction has spin projection $\sigma = +1/2$, and the spin dimer is in the single state can be written in the form

$$|\Psi_L\rangle = \sum_n [w_{n\uparrow}c_{n\uparrow}^{+}D_{00} + u_{n\uparrow}c_{n\uparrow}^{+}D_{10} + v_{n\downarrow}c_{n\downarrow}^{+}D_{11}]|0\rangle. \quad (10)$$

The admixture of triplet states of the dimer is described by the two last terms and is associated with the above-mentioned processes induced by the s–$d(f)$ exchange interaction of the electron with localized moments of the spin dimer.

We will assume that the electron ejected from the left junction has a wavevector k_L. Then the expressions for the partial amplitudes for the left ($n \le 0$) and right ($n \ge 3$) junctions can be written in the form

$$n \le 0: w_{n\uparrow} = e^{ik_L na} + r_{00}e^{-ik_L na},$$
$$u_{n\uparrow} = r_{10}e^{-iq_L na}, \quad v_{n\downarrow} = r_{11}e^{-ip_L na};$$
$$n \ge 3: w_{n\uparrow} = t_{00}e^{ik_R na}, \quad (11)$$
$$u_{n\uparrow} = t_{10}e^{iq_R na}, \quad v_{n\downarrow} = t_{11}e^{ip_R na};$$

where r_{00}, r_{10}, and r_{11} are the amplitudes emerging due to reflection from the potential structure of the dimer, which is in the singlet and triplet states, respectively; t_{00}, t_{10}, and t_{11} are the amplitudes describing transmission of the electron, in which the dimer remains in the singlet and triplet states, respectively; and k_L, k_R, q_L, q_R, p_L, and p_R are the wavevectors. The meaning of the subscripts on amplitudes r and t is analogous to that of the indices for the spin wavefunctions of the dimer. The wavevectors introduced above are connected with

the electron energy in the left junction by the dispersion relations

$$\begin{aligned} E &= \varepsilon_L + U(1) + 2t_L\cos k_L a, \\ E &= \varepsilon_L + U(1) + I + 2t_L\cos q_L a, \\ E &= \varepsilon_L + U(1) + I + (2-g_D)\mu_B H + 2t_L\cos p_L a. \end{aligned} \tag{12}$$

Analogously, we can write the following relations for the right junction:

$$\begin{aligned} E &= \varepsilon_R + U(2) + 2t_R\cos k_R a, \\ E &= \varepsilon_R + U(2) + I + 2t_R\cos q_R a, \\ E &= \varepsilon_R + U(2) + I + (2-g_D)\mu_B H + 2t_R\cos p_R a. \end{aligned} \tag{13}$$

Equating the partial amplitudes at orthogonal basis elements for $n = 0, 1, 2, 3$ in the Schrödinger equation, we obtain the missing 12 equations (A.1) with allowance for various spin configurations of the system, which are given in the Appendix.

To calculate the I–V characteristic, we must also know the solutions in the case when an electron with the spin moment projection $\sigma = +1/2$ is ejected from the right contact. In this case, relations (12) and (13) remain in force, and the wavefunction of the system can be written in the form

$$\begin{aligned} |\Psi_L\rangle = \sum_n [&w'_{n\uparrow}c^+_{n\uparrow}D_{00} + u'_{n\uparrow}c^+_{n\uparrow}D_{10} \\ &+ v'_{n\downarrow}c^+_{n\downarrow}D_{11}]|0\rangle, \end{aligned} \tag{14}$$

where

$$\begin{aligned} n \le 0\colon\ & w'_{n\uparrow} = t'_{00}e^{-ik_L na}, \\ & u'_{n\uparrow} = t'_{10}e^{-iq_L na}, \quad v'_{n\downarrow} = t'_{11}e^{-ip_L na}; \\ n \ge 3\colon\ & w'_{n\uparrow} = e^{-ik_R na} + r'_{00}e^{ik_R na}, \\ & u'_{n\uparrow} = r'_{10}e^{iq_R na}, \quad v'_{n\downarrow} = r'_{11}e^{ip_R na}. \end{aligned} \tag{15}$$

An additional system of 12 equations (A.2) is given in Appendix. In expressions (12), (13), (A.1), and (A.2), the energy is renormalized as follows: $E \longrightarrow E + 3I/4 + \mu_B H$.

It should be emphasized that our further analysis will be confined to the unimodal regime. This corresponds to the situation when an electron with a preset energy value impinging on the setup from the left (right) electrode is described by a state with a single fixed value of wavevector k_L (k_R). At the same time, for waves reflected from the setup, states with different values of wavevectors are admixed. This is due to the existence of internal degrees of freedom for the dimer setup. Owing to the s–$d(f)$ exchange interaction, the internal degrees of freedom participate in scattering and induce additional states of the system as a whole. Thus, the presence of several subbands in the energy spectrum of electrons for the entire system, which differ in quantum number values of the total spin angular momentum $\hat{J}_D$ of the dimer and its projection $\hat{J}_{Dz}$, is associated with the above-mentioned s–$d(f)$ interaction. This is a distinguishing feature of our system as compared to prevailing mesoscopic systems, in which the multimode regime of quantum wires making up the electrodes involves spatial quantization [25].

4. TRANSMISSION COEFFICIENT

The solution to the systems of equations derived above determines the reflection amplitudes r_{00}, r_{10}, and r_{11} and transmission amplitudes t_{00}, t_{10}, and t_{11}. Having evaluated these amplitudes, we can determine reflectance R and transmittance T. To this end, we use the semiclassical expressions for the incident j_{inc}, reflected j_{ref}, and transmitted j_{tr} probability flux densities:

$$\begin{aligned} j_{\text{inc}} &= \frac{1}{\hbar}\frac{\partial E}{\partial k_L}, \\ j_{\text{tr}} &= \frac{1}{\hbar}\left[\frac{\partial E}{\partial k_R}|t_{00}|^2 + \frac{\partial E}{\partial q_R}|t_{10}|^2 + \frac{\partial E}{\partial p_R}|t_{11}|^2\right], \\ j_{\text{ref}} &= \frac{1}{\hbar}\left[\frac{\partial E}{\partial k_L}|r_{00}|^2 + \frac{\partial E}{\partial q_L}|r_{10}|^2 + \frac{\partial E}{\partial p_L}|r_{11}|^2\right]. \end{aligned} \tag{16}$$

It is well known that transmittance T is defined as the ratio of the density of the transmitted probability flux to the density of the incident probability flux: $T = |j_{\text{tr}}|/|j_{\text{inc}}|$ [26]. Accordingly, we obtain

$$T = \begin{cases} T_{00} + T_{10} + T_{11}, & 0 < k_R, q_R, p_R < \pi/a \\ T_{00} + T_{10}, & 0 < k_R, q_R < \pi/a \\ T_{00}, & 0 < k_R < \pi/a, \end{cases} \tag{17}$$

where

$$\begin{aligned} T_{00} &= \frac{|t_R|}{|t_L|}\frac{\sin k_R a}{\sin k_L a}|t_{00}|^2, \\ T_{10} &= \frac{|t_R|}{|t_L|}\frac{\sin q_R a}{\sin k_L a}|t_{10}|^2, \\ T_{11} &= \frac{|t_R|}{|t_L|}\frac{\sin p_R a}{\sin k_L a}|t_{11}|^2 \end{aligned} \tag{18}$$

are the partial contributions in the total transmittance T from the states in which the dimer has the singlet or triplet spin configurations, respectively. Reflectance $R = |j_{\text{ref}}|/|j_{\text{inc}}|$ is defined as

$$R = \begin{cases} R_{00} + R_{10} + R_{11}, & 0 < k_L, q_L, p_L < \pi/a \\ R_{00} + R_{10}, & 0 < k_L, q_L < \pi/a \\ R_{00}, & 0 < k_L < \pi/a, \end{cases} \tag{19}$$

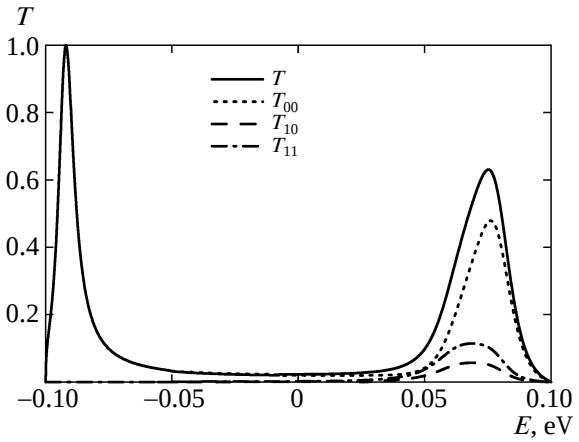

Fig. 2. Dependence of total transmittance T and its partial components T_{00}, T_{10}, and T_{11} on the energy of an incident electron for parameters $\varepsilon_L = \varepsilon_D = \varepsilon_R = 0$, $t_L = t_R = -0.05$ eV, $t_{LD} = t_{DR} = -0.025$ eV, $t_D = -0.0375$ eV, $\mu_B H = 0$, $I = 0.05$ eV, $A_{sf} = 0.15$ eV, and $V = 0$.

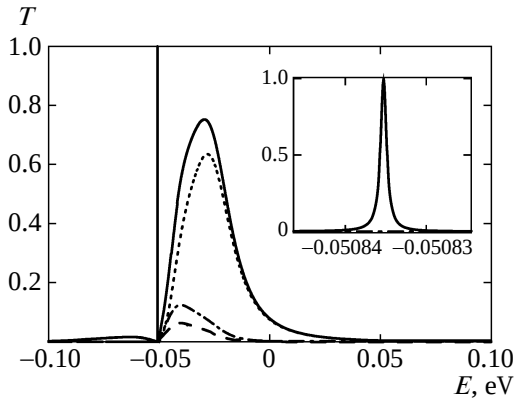

Fig. 3. Dependence of total transmittance T and its partial components T_{00}, T_{10}, and T_{11} on the energy of an incident electron for parameters $t_L = t_R = -0.05$ eV, $t_{LD} = t_{DR} = -0.025$ eV, $t_D = -0.0375$ eV, $\mu_B H = 0.25$ meV, $I = 0.05$ eV, $A_{sf} = 0.15$ eV, $\varepsilon_L = \varepsilon_R = 0$, $\varepsilon_D = -0.09$ eV, and $V = 0$. The inset shows the resonance transmittance peak induced by the magnetic field.

where

$$R_{00} = |r_{00}|^2, \quad R_{10} = \frac{\sin q_L a}{\sin k_L a}|r_{10}|^2, \qquad (20)$$
$$R_{11} = \frac{\sin p_L a}{\sin k_L a}|r_{11}|^2.$$

The number of nonzero partial contributions corresponds to the number of solutions to the dispersion equations for the wavevectors lying in the first Brillouin zone. Quantities R and T satisfy the total probability conservation law; i.e., $R + T = 1$.

Figure 2 illustrates the typical behavior of transmittance $T(E)$ and its partial components $T_{00} = T_{00}(E)$, $T_{10} = T_{10}(E)$, and $T_{11} = T_{11}(E)$ upon a change in the energy of incident electrons from the left electrode. On the $T(E)$ curve, two regions can be distinguished, in which the dependences of these quantities on energy differ substantially. In the region $E < -0.05$ eV, the total transmittance is determined only by the processes in which transitions of dimers to triplet states are not observed. For $E > -0.05$ eV, the processes leading to excitation of dimers to the triplet states come into play. For this reason, total transmittance T is formed taking into account the contributions from excited states of the electron and the dimer (dashed and dot-and-dash curves in Fig. 2).

In the region of low energies in which electrons are scattered from the potential profile of the dimer in the ground singlet state, the application of magnetic field may lead to the emergence of additional resonance peaks as shown in the inset to Fig. 3. In the case depicted in the figure, the emergence of one of two peaks in the magnetic field is demonstrated when the one-electron energy ε_D at the sites of the setup differs from analogous parameters ε_L and ε_R of the electrodes. The situation for other values of the parameters of the system is qualitatively the same. The peak at $E \approx -0.025$ eV corresponds to the right peak in Fig. 2 ($E \approx 0.075$ eV), which is shifted to the left upon an increase in the absolute value of ε_D. The effect of induction of transparency windows by the magnetic field was noted by us earlier when we considered the problems of inelastic spin-dependent electron transport by means of model spin nanostructures in continuous media [27, 28].

As can be seen from Fig. 4, the application of electric field induces noticeable changes in the heights of these peaks. In constructing the curves in Fig. 4, we assumed that the electric voltage applied to the right junction is such that $-eV = U(2) - U(1)$. Therefore, $\mu_R = \mu_L - eV$, where μ_R and μ_L are the electrochemical potentials of the right and left junctions, respectively. This assumption will be used in further analysis in calculating the current–voltage characteristics.

By varying the parameters of the system, we can obtain an energy-forbidden band (energy range $0 < E < 0.05$ eV in Fig. 5a) for the electrons in the right junction. Accordingly, the electrons incident on the dimer from the left junction and having energies from this range experience total reflection (see Fig. 5b).

5. CURRENT–VOLTAGE CHARACTERISTIC

Considering that the electron density associated with a single k state in a conductor of length L is $1/L$, we find that, in the semiclassical approximation, current I_{LR} carried by scattering state (10) is defined as ($m = 00, 10, 11$; $k_{00} = k_R$, $k_{10} = q_R$, and $k_{11} = p_R$)

$$I_{LR} = \frac{e}{L}\sum_m \sum_k \frac{1}{\hbar}\left(\frac{\partial E}{\partial k}\right)_{k = k_m} T_m(E) f_L(E), \qquad (21)$$

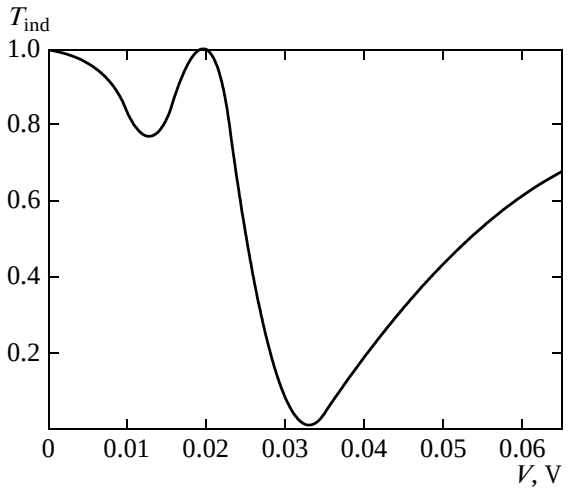

Fig. 4. Voltage dependence of the peak T_{ind} induced by the magnetic field for parameters $\varepsilon_L = \varepsilon_R = -0.05$ eV, $t_{LD} = t_{DR} = -0.025$ eV, $t_D = -0.0375$ eV, $\mu_B H = 0.25$ meV, $I = 0.1$ eV, $A_{sf} = 0.15$ eV, $\varepsilon_L = \varepsilon_R = 0.05$ eV, and $\varepsilon_D = -0.6$ eV.

where $f_L(E) \equiv f(E - \mu_L)$ is the Fermi electron distribution function. Passing from summation over quasimomentum to integration over energy, we obtain

$$I_{LR} = \frac{e}{h}\sum_m \int dE T_m(E) f_L(E). \quad (22)$$

At finite temperatures, we must take into account the electron flux from the right junction to the left one. Therefore, the current carried by states (14) can be written analogously to I_{LR}, namely,

$$I_{RL} = \frac{e}{h}\sum_m \int dE T'_m(E) f_R(E), \quad (23)$$

where $f_R(E) \equiv f(E - \mu_R)$ and T'_m are the partial transmittances for an electron incident on the setup from the right electrode, which are defined as

$$T'_{00} = \frac{|t_L|}{|t_R|}\frac{\sin k_L a}{\sin k_R a}|t'_{00}|^2,$$
$$T'_{10} = \frac{|t_L|}{|t_R|}\frac{\sin q_L a}{\sin k_R a}|t'_{10}|^2, \quad (24)$$
$$T'_{11} = \frac{|t_L|}{|t_R|}\frac{\sin p_L a}{\sin k_R a}|t'_{11}|^2.$$

The resultant current is defined by the expression

$$I = I_{LR} - I_{RL} = \frac{e}{h} \times \sum_m \int dE[T_m(E) f_L(E) - T'_m(E) f_R(E)], \quad (25)$$

which is equivalent to the formula obtained using the Landauer–Buttiker formalism [29].

Thus, electron transport in the system under investigation can be interpreted as transport through three effective channels formed due to the existence of excited states of the spin dimer. In each channel, conduction electrons have their own projections of spin moments: in two channels, their spins are polarized along the magnetic field, while in the third channel, the spins have polarization opposite to the field.

Figures 6 and 7 show the typical I–V characteristic and differential conductivity $G(V) = dI/dV$ of the setup using a spin dimer as the active element located between metal electrodes. The shape of these dependences implies that an increase in the Fermi energy in the left junction qualitatively changes the I–V characteristic. For small values of the Fermi energy at which only low-energy electrons participate in transport, the

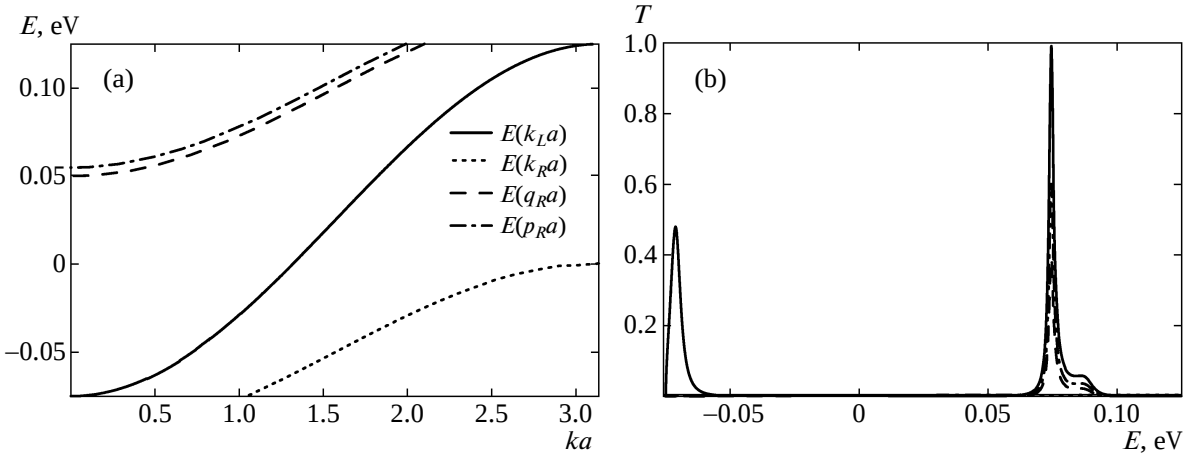

Fig. 5. (a) Band structure and (b) dependence of total transmittance T and its partial components T_{00}, T_{10}, and T_{11} on the energy of incident electron for parameters $t_L = -0.05$ eV, $t_R = -0.025$ eV, $t_{LD} = t_D = t_{DR} = -0.0125$ eV, $\mu_B H = 0.005$ eV, $I = 0.15$ eV, $A_{sf} = 0.15$ eV, $\varepsilon_L = 0.025$ eV, $\varepsilon_D = -0.0375$ eV, $\varepsilon_R = -0.05$ eV, and $V = 0$.

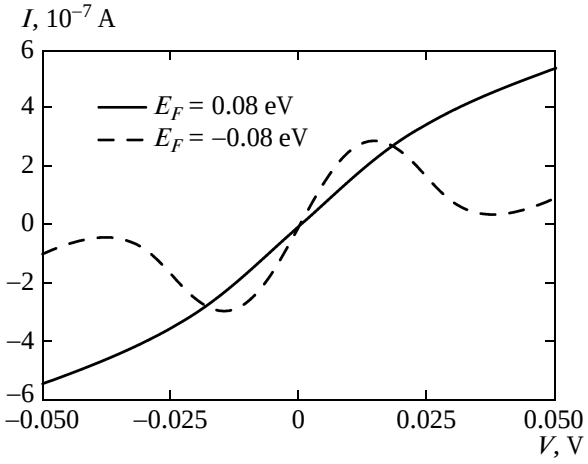

Fig. 6. Current–voltage characteristic of a spin dimer calculated for parameters $\varepsilon_L = \varepsilon_D = \varepsilon_R = 0$, $t_L = t_R = -0.05$ eV, $t_{LD} = t_{DR} = -0.025$ eV, $t_D = -0.05$ eV, $\mu_B H = 0.005$ eV, $I = 0.075$ eV, $A_{sf} = 0.125$ eV, and $T \approx 30$ K for two values of the Fermi energy of the junctions.

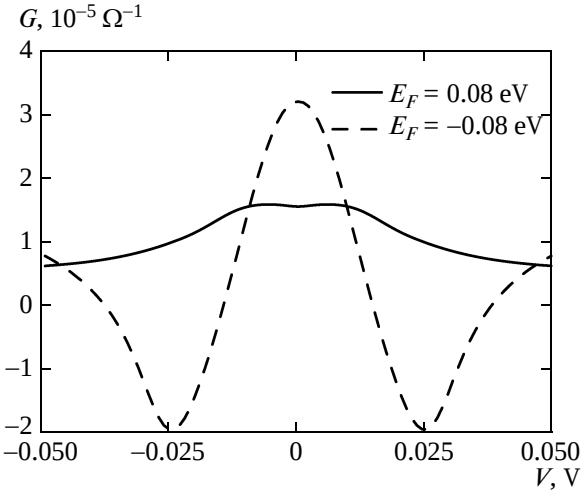

Fig. 7. Differential conductivity for a spin dimer calculated for Fig. 6.

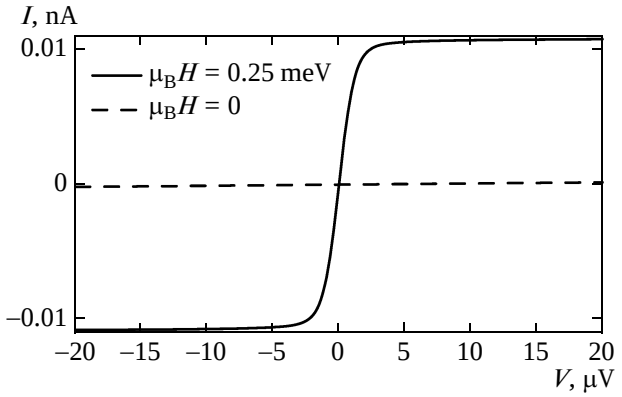

Fig. 8. Effect of magnetic field on the I–V characteristic as a result of induction of a transparency peak for parameters from Fig. 3, $E_F \approx -0.051$ eV, and $T \approx 3$ mK.

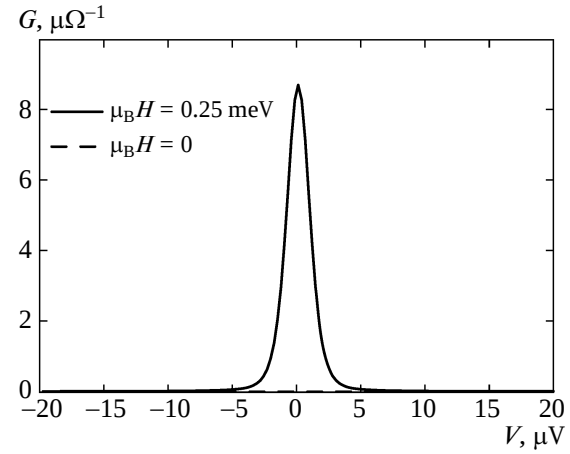

Fig. 9. Effect of magnetic field on the conductivity as a result of induction of a transparency peak for parameters from Fig. 3; $E_F \approx -0.051$ eV, and $T \approx 3$ mK.

I–V curve contains segments with a negative differential conductivity. This is observed in the regime in which triplet states of the dimer are not excited and inelastic processes are not involved. It should be noted that the emergence of regions with a negative differential conductivity was observed, in particular, in experiments using scanning electron microscopy, in which electrons were transported through molecular complexes and individual molecules adsorbed on the metal surface [30].

In the case of high Fermi energies, when the electron energy is sufficient for transition of dimers to excited states and the transport becomes inelastic, the regions with negative differential conductivity on the I–V curves disappear. In this case, the I–V characteristics correspond to Ohm's law to a high degree of accuracy.

It was mentioned above that the application of magnetic field may lead to a nontrivial change in the transport properties of the system in question. In particular, it was shown that under certain conditions, the magnetic field can induce additional transparency peaks for an electron being transported. This effect must obviously be manifested in the I–V characteristic of the system depicted in Fig. 8. It can be seen that for voltages on the order of a microvolt, the I–V characteristic exhibits a strongly nonlinear behavior and the differential conductivity shown in Fig. 9 has a sharp peak.

The above results show that in the range of parameters considered here, the system under investigation is characterized by an anomalously high magnetore-

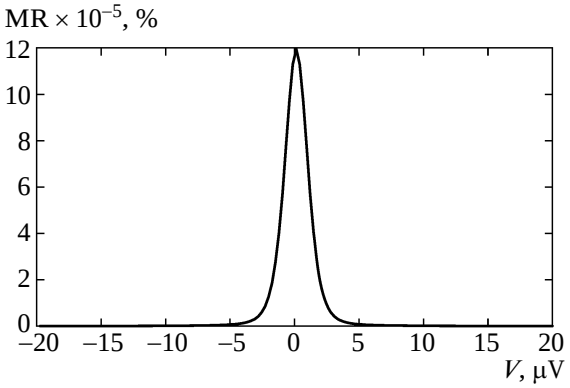

Fig. 10. Magnetoresistance for parameters from Fig. 3, $E_F \approx -0.051$ eV, and $T \approx 3$ mK.

sistance MR = $(G(H)/G(0) - 1) \times 100\%$. The corresponding calculations of the dependence of magnetoresistance on the applied voltage are illustrated in Fig. 10.

It can be seen that the change in the resistance in the magnetic field can amount to $10^5\%$. It should be noted that high values of the magnetoresistance are observed quite frequently for the setups based on nanostructural elements.

6. CONCLUSIONS

The above analysis of quantum electron transport through the spin-dimer system has made it possible to establish a number of features associated with the internal degrees of freedom in the system. The main feature is that the potential profile for an electron being transported is formed due to the s–$d(f)$ exchange interaction between the spin moments of the electron and of the nanostructure. Therefore, for the singlet state of the dimer, in which the spin configuration is described by a coherent superposition of states with different values of the spin moment projections on the quantization axis, the Ising part of the s–$d(f)$ exchange interaction leads to the formation of a combination of potential profiles of the barrier–well, well–barrier, etc. types. A specific realization of these profiles is determined by the spin polarization of the electron being transported. This induces the spin-polarization dependence of the transport characteristics of the nanostructure under investigation. The transverse part of the s–$d(f)$ exchange interaction induces a transition of the spin dimer from the singlet state to excited triplet states with a simultaneous change in the potential profile of the structure. It is these effects that are responsible for significant modifications of the transport characteristics of nanostructures upon an increase in the electron energy and application of a magnetic field.

The admixture of excited triplet states of the dimer subsystem leads to the formation of additional channels both in the states reflected from the structure, and in the states determining the contribution to the transmittance. In such channels, the values of quasi-momenta for electron waves may differ substantially from the quasi-momentum of the electron incident on the structure due to the exchange interaction in the dimer subsystem. In this case, the transport characteristics of the system under investigation are determined by the coherent superposition of states with several quasi-momenta.

These effects determine the features of the current–voltage characteristic of the spin-dimer system. One of these features is associated with disappearance of the negative differential conductivity upon an increase in the Fermi energy. It should be emphasized that the I–V characteristic contains segments with a negative differential conductivity only when the Fermi energy is relatively low and the kinetic energy of electrons is insufficient for exciting the dimer subsystem. For high values of the Fermi energy, when electrons can transform spin dimers to excited state and initiate the above-mentioned additional transport channels, the differential conductivity becomes positive everywhere.

Concluding the section, let us consider the effect associated with the emergence of additional transparency peaks induced in the spectral characteristic of the system by a magnetic field. It was shown in the concluding section of this article that this effect results in a qualitative modification of the I–V characteristic of the system and the emergence of colossal magnetoresistance. As noted above, the additional transparency peaks appear in a magnetic field only when the spin-flip processes are taken into account. This leads to the conclusion that in analyzing the effects of spin-dependent transport associated with the interaction of passing electron with the spin degrees of freedom of the scattering structure, allowance for the processes leading to a change in the spin configuration of the nanostructure may be of fundamental importance in fabricating scattering nanostructures with colossal magnetoresistance.

ACKNOWLEDGMENTS

This study was carried out under the program of the Physical Science Department of the Russian Academy of Sciences, Federal Target Program "Scientific and Scientific–Pedagogical Personnel of Innovative Russia in 2009–2013," Interdisciplinary Integration project no. 53 of the Siberian Branch of the Russian Academy of Sciences, and under partial support from the Russian Foundation for Basic Research (project no. 09-02-00127). The research work of one of the authors (S.V.A) was supported by grant no. MK-1300.2011.2 from the President of the Russian Federation.

APPENDIX

System of Equations for Amplitudes

In the case when an electron with a spin of 1/2 is incident from the left electrode on the dimer in the singlet state, the system of equations for the transmission and reflection amplitudes has the form

$$
\begin{aligned}
&t_L(e^{-ik_La} + r_{00}e^{ik_La}) \\
&+ (\varepsilon_L + U(1) - E)(1 + r_{00}) + t_{LD}w_{1\uparrow} = 0, \\
&t_{LD}(1 + r_{00}) + (\varepsilon_D + U(1) - E)w_{1\uparrow} \\
&+ \frac{A_{sf}u_{1\uparrow}}{4} - \frac{A_{sf}V_{1\downarrow}}{2\sqrt{2}} + t_Dw_{2\uparrow} = 0, \\
&t_Dw_{1\uparrow} + (\varepsilon_D + U(2) - E)w_{2\uparrow} \\
&- \frac{A_{sf}u_{2\uparrow}}{4} + \frac{A_{sf}V_{2\downarrow}}{2\sqrt{2}} + t_{DR}t_{00}e^{3ik_Ra} = 0, \\
&t_{DR}w_{2\uparrow} + (\varepsilon_R + U(2) - E)t_{00}e^{3ik_Ra} + t_Rt_{00}e^{4ik_Ra} = 0, \\
&t_Lr_{10}e^{iq_La} + (\varepsilon_L + U(1) + I - E)r_{10} + t_{LD}u_{1\uparrow} = 0, \\
&t_{LD}r_{10} + (\varepsilon_D + U(1) + I - E)u_{1\uparrow} \\
&+ \frac{A_{sf}w_{1\uparrow}}{4} + \frac{A_{sf}V_{1\downarrow}}{2\sqrt{2}} + t_Du_{2\uparrow} = 0, \\
&t_Du_{1\uparrow} + (\varepsilon_D + U(2) + I - E)u_{2\uparrow} \\
&- \frac{A_{sf}w_{2\uparrow}}{4} + \frac{A_{sf}V_{2\downarrow}}{2\sqrt{2}} + t_{DR}t_{10}e^{3iq_Ra} = 0, \\
&t_{DR}u_{2\uparrow} + (\varepsilon_R + U(2) + I - E)t_{10}e^{3iq_Ra} + t_Rt_{10}e^{4iq_Ra} = 0, \\
&t_Lr_{11}e^{ik_{11}La} + (\varepsilon_L + U(1) + (2 - g_D)\mu_BH \\
&+ I - E)r_{11} + t_{LD}V_{1\downarrow} = 0, \\
&t_{LD}r_{11} + \left(\varepsilon_D + U(1) + (2 - g_D)\mu_BH + I - \frac{A_{sf}}{4} - E\right)V_{1\downarrow} \\
&+ \frac{A_{sf}}{2\sqrt{2}}(u_{1\uparrow} - w_{1\uparrow}) + t_DV_{2\downarrow} = 0, \\
&t_DV_{1\downarrow} + \left(\varepsilon_D + U(2) + (2 - g_D)\mu_BH + I - \frac{A_{sf}}{4} - E\right)V_{2\downarrow} \\
&+ \frac{A_{sf}}{2\sqrt{2}}(u_{2\uparrow} + w_{2\uparrow}) + t_{DR}t_{11}e^{3ip_Ra} = 0, \\
&t_{DR}V_{2\downarrow} + (\varepsilon_R + U(2) + (2 - g_D)\mu_BH \\
&+ I - E)t_{11}e^{3ip_Ra} + t_Rt_{11}e^{4ip_Ra} = 0.
\end{aligned}
\tag{A.1}
$$

Analogously, in the situation when an electron with a spin of 1/2 is incident from the right electrode on the dimer in the singlet state, the system of equations for the transmission and reflection amplitudes can be written in the form

$$
\begin{aligned}
&t_Lt'_{00}e^{ik_La} + (\varepsilon_L + U(1) - E)t'_{00} + t_{LD}w_{1\uparrow} = 0, \\
&t_{LD}t'_{00} + (\varepsilon_D + U(1) - E)w_{1\uparrow} \\
&+ \frac{A_{sf}u_{1\uparrow}}{4} - \frac{A_{sf}V_{1\downarrow}}{2\sqrt{2}} + t_Dw_{2\uparrow} = 0, \\
&t_Dw_{1\uparrow} + (\varepsilon_D + U(2) - E)w_{2\uparrow} - \frac{A_{sf}u_{2\uparrow}}{4} \\
&+ \frac{A_{sf}V_{2\downarrow}}{2\sqrt{2}} + t_{DR}(e^{-3ik_Ra} + r'_{00}e^{3ik_Ra}) = 0, \\
&t_{DR}w_{2\uparrow} + (\varepsilon_R + U(2) - E)(e^{-3ik_Ra} + r'_{00}e^{3ik_Ra}) \\
&+ t_R(e^{-4ik_Ra} + r'_{00}e^{4ik_Ra}) = 0, \\
&t_Lt'_{10}e^{iq_La} + (\varepsilon_L + U(1) + I - E)t'_{10} + t_{LD}u_{1\uparrow} = 0, \\
&t_{LD}t'_{10} + (\varepsilon_D + U(1) + I - E)u_{1\uparrow} \\
&+ \frac{A_{sf}w_{1\uparrow}}{4} + \frac{A_{sf}V_{1\downarrow}}{2\sqrt{2}} + t_Du_{2\uparrow} = 0, \\
&t_Du_{1\uparrow} + (\varepsilon_D + U(2) + I - E)u_{2\uparrow} \\
&- \frac{A_{sf}w_{2\uparrow}}{4} + \frac{A_{sf}V_{2\downarrow}}{2\sqrt{2}} + t_{DR}r'_{10}e^{3iq_Ra} = 0, \\
&t_{DR}u_{2\uparrow} + (\varepsilon_R + U(2) + I - E)r'_{10}e^{3iq_Ra} \\
&+ t_Rr'_{10}e^{4iq_Ra} = 0, \\
&t_Lt'_{11}e^{ip_La} + (\varepsilon_L + U(1) + (2 - g_D)\mu_BH \\
&+ I - E)t'_{11} + t_{LD}V_{1\downarrow} = 0, \\
&t_{LD}t'_{11} + \left(\varepsilon_D + U(1) + (2 - g_D)\mu_BH + I - \frac{A_{sf}}{4} - E\right)V_{1\downarrow} \\
&+ \frac{A_{sf}}{2\sqrt{2}}(u_{1\uparrow} - w_{1\uparrow}) + t_DV_{2\downarrow} = 0, \\
&t_DV_{1\downarrow} + \left(\varepsilon_D + U(2) + (2 - g_D)\mu_BH + I - \frac{A_{sf}}{4} - E\right)V_{2\downarrow} \\
&+ \frac{A_{sf}}{2\sqrt{2}}(u_{2\uparrow} + w_{2\uparrow}) + t_{DR}r'_{11}e^{3ip_Ra} = 0, \\
&t_{DR}V_{2\downarrow} + (\varepsilon_R + U(2) + (2 - g_D)\mu_BH \\
&+ I - E)r'_{11}e^{3ip_Ra} + t_Rr'_{11}e^{4ip_Ra} = 0.
\end{aligned}
\tag{A.2}
$$

REFERENCES

1. C. J. Gorter, Physica (Amsterdam) **17**, 777 (1951).
2. K. K. Likharev, IBM J. Res. Dev. **32**, 144 (1988).
3. H. Ishikuro, T. Fujii, T. Saraya, G. Hashiguchi, T. Hiramoto, and T. Ikoma, Appl. Phys. Lett. **68**, 3585 (2009).
4. M. Galperin, M. A. Ratner, and A. Nitzan, Phys. Rev. B: Condens. Matter **74**, 075326 (2006).
5. T. Frederiksen, M. Paulsson, M. Brandbyge, and A.-P. Jauho, Phys. Rev. B: Condens. Matter **75**, 205413 (2007).

6. M. Galperin, M. A. Ratner, A. Nitzan, and A. Troisi, Science (Washington) **319**, 1056 (2008).
7. P. I. Arseev and N. S. Maslova, Usp. Fiz. Nauk **180** (11), 1197 (2010) [Phys.—Usp. **53** (11), 1151 (2010)].
8. J. M. Tour, *Molecular Electronics: Commercial Insights, Chemistry, Devices, Architecture, and Programming* (World Scientific, Singapore, 2003).
9. G. A. Prinz et al., Science (Washington) **282**, 1660 (1998).
10. S. A. Wolf, D. D. Awschalom, R. A. Buhrman, J. M. Daughton, S. von Molnár, M. L. Roukes, A. Y. Chtchelkanova, and D. M. Treger, Science (Washington) **294**, 1488 (2001).
11. J. C. Slonczewski, J. Magn. Magn. Mater. **159**, L1 (1996).
12. L. Berger, Phys. Rev. B: Condens. Matter **54**, 9353 (1996).
13. Yu. V. Gulyaev, P. E. Zil'berman, E. M. Epshtein, and R. J. Elliott, Zh. Eksp. Teor. Fiz. **127** (5), 1138 (2005) [JETP **100** (5), 1005 (2005)].
14. Yu. V. Gulyaev, P. E. Zilberman, A. I. Panas, and E. M. Epshtein, Zh. Eksp. Teor. Fiz. **134** (6), 1200 (2008) [JETP **107** (6), 1027 (2008)].
15. A. J. Heinrich, J. A. Gupta, C. P. Lutz, and D. M. Eigler, Science (Washington) **306**, 466 (2004).
16. C. F. Hirjibehedin, C. P. Lutz, and A. J. Heinrich, Science (Washington) **312**, 1021 (2006).
17. C. F. Hirjibehedin, C.-Y. Lin, A. F. Otte, M. Ternes, C. P. Lutz, B. A. Jones, and A. J. Heinrich, Science (Washington) **317**, 1199 (2007).
18. J. Fernández-Rossier, Phys. Rev. Lett. **102**, 256802 (2009).
19. G.-Y. Sun, C.-X. Wu, Y. Chen, and Z.-L. Yang, Eur. Phys. J. B **49**, 459 (2006).
20. R.-Q. Wang, Y.-Q. Zhou, B. Wang, and D. Y. Xing, Phys. Rev. B: Condens. Matter **75**, 045318 (2007).
21. P. Gambardella, S. Rusponi, M. Veronese, S. S. Dhesi, C. Grazioli, A. Dallmeyer, I. Cabria, R. Zeller, P. H. Dederichs, K. Kern, C. Carbone, and H. Brune, Science (Washington) **300**, 1130 (2003).
22. D. Gatteschi, R. Sessoli, and J. Villain, *Molecular Nanomagnets* (Oxford University Press, Oxford, 2006).
23. R. Landauer, IBM J. Res. Dev. **1**, 223 (1957).
24. M. Büttiker, IBM J. Res. Dev. **32**, 317 (1988).
25. H. Bruus and K. Flensberg, *Many-Body Quantum Theory in Condensed Matter Physics: An Introduction* (Oxford University Press, Oxford, 2004).
26. L. D. Landau and E. M. Lifshitz, *Course of Theoretical Physics*, Vol. 3: *Quantum Mechanics: Non-Relativistic Theory* (Nauka, Moscow, 2001; Butterworth–Heinemann, Oxford, 2002).
27. V. V. Val'kov and S. V. Aksenov, Izv. Akad. Nauk, Ser. Fiz. **74** (1), 6 (2010) [Bull. Russ. Acad. Sci.: Phys. **74** (1), 1 (2010)].
28. V. V. Val'kov and S. V. Aksenov, Izv. Akad. Nauk, Ser. Fiz. **74** (5), 763 (2010) [Bull. Russ. Acad. Sci.: Phys. **74** (5), 731 (2010)].
29. S. Datta, *Electronic Transport in Mesoscopic Systems* (Cambridge University Press, Cambridge, 1995).
30. J. M. Seminario, *Molecular and Nano Electronics: Analysis, Design, and Simulation* (Elsevier, Amsterdam, The Netherlands, 2007).

Translated for N. Wadhwa